Analytic solution for a higher-order lattice Boltzmann method: Slip velocity and Knudsen layer

Seung Hyun Kim* and Heinz Pitsch
Department of Mechanical Engineering, Stanford University, California 94305-3035, USA
(Received 30 January 2008; revised manuscript received 22 April 2008; published 17 July 2008)

We present the analysis of a higher-order lattice Boltzmann (LB) method based on the fourth-order Gauss-Hermite quadrature, with emphasis on the slip velocity and the Knudsen layer. The exact solution of the slip velocity for the higher-order LB equation is obtained for Poiseuille flows with finite Knudsen numbers. Due to increased accuracy in velocity space discretization, the higher-order scheme gives much improved slip coefficients as compared with the standard LB method based on the third-order Gauss-Hermite quadrature. A multiple relaxation time model is investigated to show the effects of the relaxation times for higher-order moments on the slip phenomena.

DOI: 10.1103/PhysRevE.78.016702 PACS number(s): 47.11.−j, 47.61.−k, 05.20.Dd

I. INTRODUCTION

With the advancement of microtechnology and nanotechnology, fluid flows at the micrometer and nanometer scale have recently attracted significant attention [1,2]. The major characteristics of flows in this regime are the presence of the slip velocity and the growing importance of the kinetic layer, where the Navier-Stokes equations break down [2]. While the Boltzmann equation [3] can accurately describe the strong nonequilibrium effects in the kinetic layer for gaseous flows, the development of a more efficient, reduced-order model has been a challenging problem.

The lattice Boltzmann (LB) method [4–8], as a reduced-order model of the Boltzmann equation, has been successfully applied to various problems including multicomponent, multiphase, and other complex flows. While the LB method is designed originally to mimic the Navier-Stokes hydrodynamics, significant progress in the modeling of microscale and nanoscale flows has recently been made [9–13]. Since fluid-wall interactions play a crucial role in finite Knudsen number (Kn) flows, the major focus has been on boundary conditions to capture the slip phenomena [9,10,12,14]. Kinetic boundary conditions [10], together with the modification of the relaxation dynamics, have been proposed, which can reproduce the slip phenomena up to second order in Kn [14–16]. However, due to the lattice constraint, the slip coefficients of the standard LB equation, which are based on the third-order Gauss-Hermite quadrature, are found to be slightly larger than those of the Boltzmann equation when the diffuse scattering boundary condition is used for both methods [16].

The LB method can be based on a higher-order quadrature in order to increase the accuracy of discretization in velocity phase space [17,18]. For moderate Kn flows beyond the slip flow regime, the higher-order LB method is needed to obtain a quantitative prediction as well as to reproduce the presence of the Knudsen layer [17,18]. Ansumali *et al.* [17] presented analytical solutions for Couette flows for a hierarchy of the LB method and showed that the increase of order in the Gauss-Hermite quadrature results in a much more accurate treatment of finite Kn flows. Szalmas [19] showed that the width of the Knudsen layer can be adjusted in the multiple relaxation time (MRT) model obtained from the fourth-order Gauss-Hermite quadrature [20,21].

In this paper, we present the analysis of a higher-order LB method with emphasis on the slip velocity and the Knudsen layer. Using the moment method of Ansumali *et al.* [17], the exact solution of the slip velocity for the higher-order LB equation based on the fourth-order Gauss-Hermite quadrature is obtained for finite Kn Poiseuille flows. The analysis of a MRT model is presented to show the effects of the relaxation dynamics of higher-order moments on the slip velocity and the Knudsen layer.

II. LATTICE BOLTZMANN METHOD

The discrete velocity Boltzmann (DVB) equation with a single relaxation time Bhatnagar-Gross-Krook (BGK) collision operator [7] can be written as

$$\partial_t f_i + c_{i\alpha}\partial_\alpha f_i = -\frac{1}{\tau}(f_i - f_i^{\mathrm{eq}}) + F_i, \tag{1}$$

where f_i is the distribution function of the discrete velocity $c_{i\alpha}$, t is time, α is the spatial coordinate, τ is the relaxation time, and F_i is an external force for the velocity $c_{i\alpha}$. The equilibrium distribution function and the external force term are, respectively, given by [18]

$$f_i^{\mathrm{eq}} = w_i\left[\rho + \frac{j_\alpha c_{i\alpha}}{c_s^2} + \frac{1}{2}\frac{(j_\alpha c_{i\alpha})^2}{\rho c_s^4} - \frac{1}{2}\frac{j_\alpha j_\alpha}{\rho c_s^2}\right], \tag{2}$$

$$F_i = w_i\rho\left[\frac{g_\alpha c_{i\alpha}}{c_s^2} + \frac{g_\alpha u_\beta c_{i\alpha} c_{i\beta}}{c_s^4} - \frac{g_\alpha u_\alpha}{c_s^2}\right], \tag{3}$$

where g_α is the external body force, w_i is the weight for the discrete velocity $c_{i\alpha}$, and $c_s(=\sqrt{RT_0})$ is the sound speed. R is the gas constant and T_0 is the reference temperature. The density ρ and the momentum density j_α are, respectively, given by

$$\sum_i f_i = \rho, \tag{4}$$

*shkcomb@stanford.edu

$$\sum_i c_{i\alpha} f_i = j_\alpha = \rho u_\alpha. \tag{5}$$

In the standard LB method, the discrete velocities $c_{i\alpha}$ are based on the third-order Gauss-Hermite quadrature, where the abscissas are zeros of the third-order Hermite polynomials, in order to recover the (isothermal) Navier-Stokes equations in the small Kn limit. Here, we use the next member of the Gauss-Hermite quadrature. The fourth-order Gauss-Hermite quadrature has the quadrature points $\{\pm a, \pm b\}$, with the weights $\{w_a, w_b\}$, where $a=\sqrt{3-\sqrt{6}}$ and $b=\sqrt{3+\sqrt{6}}$ [22]. The two-dimensional (2D) quadrature D2Q16 can be obtained by the product formula [18,22]. Here, the discrete velocities are given by

$$c_{ix} = c_s\{a,-a,b,-b,a,-a,b,-b,a,-a,b,-b,a,-a,b,-b\}, \tag{6}$$

$$c_{iy} = c_s\{a,a,a,a,-a,-a,-a,-a,b,b,b,b,-b,-b,-b,-b\}. \tag{7}$$

The equilibrium function for D2Q16 can be constructed to satisfy the H theorem in discrete phase space [22] or by the third-order Hermite expansion of the Maxwellian distribution [18]. Here, of primary interest are low Mach number flows and for simplicity, terms up to second order are retained in Eq. (2). Using the Chapman-Enskog expansion, the kinematic viscosity is obtained as $\nu=\tau c_s^2$. The equation of state is $p=c_s^2\rho$, where p is the pressure.

The LB equation is obtained by the time and spatial discretization of the DVB equation [7]. The errors due to the time and spatial discretization vanishes when $\delta_x \to 0$, where δ_x is the lattice spacing. Since the LB equation is consistent with the DVB equation, the DVB equation will also be referred to as the LB equation, hereafter, for convenience.

III. ANALYTIC SOLUTION FOR POISEUILLE FLOW

An analytic solution of the D2Q16 LB equation is obtained for Poiseuille flow. The solution method is based on that of Ansumali *et al.* [17], where a moment system corresponding to the LB equation is solved. The moment system for D2Q16 [23] can be written as

$$\begin{aligned} m_j &= \sum_i e_{j,i} f_i \\ &= \{\rho, j_x, j_y, P_{xx}, P_{xy}, P_{yy}, Q_{xyy}, Q_{yxx}, Q_{xxx}, Q_{yyy}, \\ &\quad R_x, R_y, R, S_x, S_y, T\}, \end{aligned} \tag{8}$$

where

$$\begin{aligned} e_{j,i} = \{&1, c_{ix}, c_{iy}, c_{ix}c_{ix}, c_{ix}c_{iy}, c_{iy}c_{iy}, c_{ix}c_{iy}^2, \\ &c_{iy}c_{ix}^2, c_{ix}^3, c_{iy}^3, (c_{ix}^2 - 3c_s^2)c_{ix}c_{iy}, (c_{iy}^2 - 3c_s^2)c_{ix}c_{iy}, \\ &(c_{ix}^2 - c_s^2)(c_{iy}^2 - c_s^2), c_{ix}(c_{ix}^2 - 3c_s^2)(c_{iy}^2 - 3c_s^2), \\ &c_{iy}(c_{ix}^2 - 3c_s^2)(c_{iy}^2 - 3c_s^2), c_{ix}c_{iy}(c_{ix}^2 - 3c_s^2)(c_{iy}^2 - 3c_s^2)\}. \end{aligned} \tag{9}$$

In force-driven Poiseuille flow, the flow is steady, $\partial_t(\cdot)=0$, and unidirectional, $\partial_x(\cdot)=0$. For impermeable walls, which are located at $y=H/2$ and $-H/2$, the density is uniform and $j_y=0$. The velocity u_x can be obtained by solving the following moment equations:

$$\partial_y P_{xy} = \rho g, \tag{10}$$

$$\partial_y Q_{xyy} = -\frac{1}{\tau} P_{xy}, \tag{11}$$

$$\partial_y (R_y + 3c_s^2 P_{xy}) = -\frac{1}{\tau}(Q_{xyy} - c_s^2 j_x) + c_s^2 \rho g, \tag{12}$$

$$\partial_y (6c_s^2 Q_{xyy} - 3c_s^4 j_x) = -\frac{1}{\tau}(R_y + 3c_s^2 P_{xy}). \tag{13}$$

From Eqs. (10)–(13), we obtain

$$P_{xy} = \rho g y, \tag{14}$$

$$Q_{xyy} - c_s^2 j_x = -5\tau c_s^2 \rho g - 3\tau^2 c_s^4 \partial_y^2 j_x, \tag{15}$$

$$R_y = 3c_s^2 P_{xy} + 3\tau c_s^4 \partial_y j_x, \tag{16}$$

where the symmetry of the flow at $y=0$ is used. In the present problem, the moments involving even powers of c_{iy} are symmetric about $y=0$, while those involving odd powers of c_{iy} are antisymmetric about $y=0$. The equation for j_x reads

$$-3\tau^3 c_s^4 \partial_y^4 j_x + \tau c_s^2 \partial_y^2 j_x = -\rho g. \tag{17}$$

The first term on the left-hand side of Eq. (17) is responsible for the Knudsen layer, which is not captured in the standard D2Q9 LB method [16,17].

The solution for j_x can be written as

$$j_x = -\frac{1}{2\tau c_s^2}\rho g y^2 + A \cosh\left(\frac{1}{\sqrt{3\tau}c_s} y\right) + B, \tag{18}$$

where the symmetry of the flow at $y=0$ is used again. The integration constants A and B can be obtained from the boundary condition of the distribution functions. At the bottom wall, the particles are assumed to be reflected diffusely. The kinetic boundary condition with diffuse scattering kernel [10] can be written as

$$f_i|_{y=-H/2} = \Psi f_i^{\mathrm{eq}}(\rho_w, j_{\alpha w}) \quad \text{for} \quad c_{iy} > 0, \tag{19}$$

where

$$\Psi = \frac{\sum_{(c_{j\alpha}-u_{\alpha w})n_\alpha < 0} |(c_{j\alpha} - u_{\alpha w})n_\alpha| f_j|_{y=-H/2}}{\sum_{(c_{j\alpha}-u_{\alpha w})n_\alpha < 0} |(c_{k\alpha} - u_{\alpha w})n_\alpha| f_k^{\mathrm{eq}}(\rho_w, j_{\alpha w})}. \tag{20}$$

Here, n_α is the inward wall-normal vector, $\rho_w=\rho$, and $j_{\alpha w}$ is the momentum density evaluated using the velocity of the wall, $u_{\alpha w}$. For the present problem, the diffuse scattering boundary condition reduces to (see the Appendix)

$$f_i|_{y=-H/2} = f_i^{\mathrm{eq}}(\rho, j_{xw}, j_{yw}) = \rho w_i \quad \text{for} \quad c_{iy} > 0. \tag{21}$$

The nonequilibrium distribution function at the wall is then given by

$$f_i^{\mathrm{neq}}|_{y=-H/2} = \rho w_i - f_i^{\mathrm{eq}}(\rho, j_x|_{y=-H/2}, 0) \quad \text{for} \quad c_{iy} > 0. \tag{22}$$

Using Eq. (22), we obtain

$$\begin{aligned}
&[a(f_1^{\mathrm{neq}} - f_2^{\mathrm{neq}}) + b(f_3^{\mathrm{neq}} - f_4^{\mathrm{neq}})]_{y=-H/2} \\
&= -2w_a(w_a a^2 + w_b b^2)\frac{j_x|_{y=-H/2}}{c_s} \\
&= -2w_a(w_a a^2 + w_b b^2)\frac{1}{c_s} \\
&\quad \times \left[-\rho g \frac{H^2}{8\tau c_s^2} + A\cosh\left(-\frac{\alpha}{2}\right) + B \right],
\end{aligned} \tag{23}$$

$$\begin{aligned}
&[a(f_9^{\mathrm{neq}} - f_{10}^{\mathrm{neq}}) + b(f_{11}^{\mathrm{neq}} - f_{12}^{\mathrm{neq}})]_{y=-H/2} \\
&= -2w_b(w_a a^2 + w_b b^2)\frac{j_x|_{y=-H/2}}{c_s} \\
&= -2w_b(w_a a^2 + w_b b^2)\frac{1}{c_s} \\
&\quad \times \left[-\rho g \frac{H^2}{8\tau c_s^2} + A\cosh\left(-\frac{\alpha}{2}\right) + B \right],
\end{aligned} \tag{24}$$

where $\alpha = H/(\sqrt{3}\tau c_s)$. Alternatively, the nonequilibrium distribution function can be obtained using the linear relationship between the distribution functions and the moments as follows:

$$f_i^{\mathrm{neq}} = \sum_j e_{j,i}^{-1} m_j^{\mathrm{neq}}, \tag{25}$$

where

$$e_{j,i}^{-1} = \frac{w_i}{\sum_k w_k e_{j,k} \bar{e}_{j,k}} \bar{e}_{j,i}. \tag{26}$$

Here, $\bar{e}_{j,i}$ is orthogonal to $e_{j,i}$, with respect to the weight w_i and can be obtained by a procedure similar to the Gram-Schmidt orthogonalization. The superscript neq represents the nonequilibrium part of the quantity. Using Eq. (25), we obtain

$$\begin{aligned}
&[a(f_1^{\mathrm{neq}} - f_2^{\mathrm{neq}}) + b(f_3^{\mathrm{neq}} - f_4^{\mathrm{neq}})]_{y=-H/2} \\
&= 2w_a(w_a a^2 + w_b b^2) \\
&\quad \times \left[\frac{P_{xy}^{\mathrm{neq}}}{c_s^2} a + \frac{Q_{xyy}^{\mathrm{neq}}}{2c_s^3}(a^2 - 1) + \frac{R_y^{\mathrm{neq}}}{6c_s^4} a(a^2 - 3) \right]_{y=-H/2} \\
&= 2w_a(w_a a^2 + w_b b^2)\left\{ -\frac{\rho g H}{2c_s^2} a \right. \\
&\quad + \left[-\frac{\tau\rho g}{c_s} - \frac{A}{2c_s}\cosh\left(-\frac{\alpha}{2}\right) \right](a^2 - 1) \\
&\quad \left. + \frac{A}{2\sqrt{3}c_s}\sinh\left(-\frac{\alpha}{2}\right) a(a^2 - 3) \right\},
\end{aligned} \tag{27}$$

$$\begin{aligned}
&[a(f_9^{\mathrm{neq}} - f_{10}^{\mathrm{neq}}) + b(f_{11}^{\mathrm{neq}} - f_{12}^{\mathrm{neq}})]_{y=-H/2} \\
&= 2w_b(w_a a^2 + w_b b^2) \\
&\quad \times \left[\frac{P_{xy}^{\mathrm{neq}}}{c_s^2} b + \frac{Q_{xyy}^{\mathrm{neq}}}{2c_s^3}(b^2 - 1) + \frac{R_y^{\mathrm{neq}}}{6c_s^4} b(b^2 - 3) \right]_{y=-H/2} \\
&= 2w_b(w_a a^2 + w_b b^2)\left\{ -\frac{\rho g H}{2c_s^2} b \right. \\
&\quad + \left[-\frac{\tau\rho g}{c_s} - \frac{A}{2c_s}\cosh\left(-\frac{\alpha}{2}\right) \right](b^2 - 1) \\
&\quad \left. + \frac{A}{2\sqrt{3}c_s}\sinh\left(-\frac{\alpha}{2}\right) b(b^2 - 3) \right\}.
\end{aligned} \tag{28}$$

Comparing Eqs. (23) and (24) and Eqs. (27) and (28), we obtain

$$\begin{aligned}
&\left[\sqrt{\frac{3}{2}}\cosh\left(\frac{\alpha}{2}\right) + \frac{a}{\sqrt{2}}\sinh\left(\frac{\alpha}{2}\right) \right] A + B \\
&\quad = \frac{\rho g H^2}{8\tau c_s^2} + \frac{\rho g H}{2c_s} a + \tau\rho g(a^2 - 1),
\end{aligned} \tag{29}$$

$$\begin{aligned}
&\left[-\sqrt{\frac{3}{2}}\cosh\left(\frac{\alpha}{2}\right) - \frac{b}{\sqrt{2}}\sinh\left(\frac{\alpha}{2}\right) \right] A + B \\
&\quad = \frac{\rho g H^2}{8\tau c_s^2} + \frac{\rho g H}{2c_s} b + \tau\rho g(b^2 - 1),
\end{aligned} \tag{30}$$

from which the constants A and B are given by

$$A = -\frac{\rho g H/c_s (b - a)/\sqrt{2} + 4\sqrt{3}\tau\rho g}{2\sqrt{3}\cosh(\alpha/2) + (a + b)\sinh(\alpha/2)}, \tag{31}$$

$$B = \frac{b - a}{2\sqrt{2}}\sinh\left(\frac{\alpha}{2}\right) A + \frac{\rho g H^2}{8\tau c_s} + \frac{\rho g H}{4c_s}(a + b) + 2\tau\rho g. \tag{32}$$

The normalized velocity is thus given by

$$\hat{u}_x = -\hat{y}^2 + \frac{1}{4} + \hat{A}\phi(\alpha\hat{y}) + \hat{B}, \tag{33}$$

where

$$\hat{A} = -\frac{2(b - a)/\sqrt{6}\alpha^{-1} + 8/\sqrt{3}\alpha^{-2}}{2\sqrt{3}\phi(\alpha/2) + (a + b)\varphi(\alpha/2)}, \tag{34}$$

$$\begin{aligned}
\hat{B} &= \left[\frac{a + b}{2\sqrt{3}} - \frac{1}{2\sqrt{3}}\frac{(b - a)^2\varphi(\alpha/2)}{2\sqrt{3}\phi(\alpha/2) + (a + b)\varphi(\alpha/2)} \right]\alpha^{-1} \\
&\quad + \left(\frac{4}{3} - \frac{4}{\sqrt{6}}\frac{(b - a)\varphi(\alpha/2)}{2\sqrt{3}\phi(\alpha/2) + (a + b)\varphi(\alpha/2)} \right)\alpha^{-2}.
\end{aligned} \tag{35}$$

Here, $\hat{u}_x = 2\nu/(gH^2)u_x$, $\hat{y} = y/H$, $\phi(x) = \cosh(x)e^{-\alpha/2}$ and $\varphi(x) = \sinh(x)e^{-\alpha/2}$.

In Poiseuille flow, of primary interest is the dependence of the total mass flow rate, normalized by a pressure gradient, on Kn. Here, Kn is based on the viscosity-based mean free path [2,3,16]: $\mathrm{Kn}=\sqrt{\pi/2}(\tau c_s)/H$. The rarefaction parameter α is thus related to Kn as $\alpha=\sqrt{\pi}/6\mathrm{Kn}^{-1}$. For D2Q16, the normalized mass flow rate is given by

$$Q=\frac{1}{6\mathrm{Kn}}+C_1+C_2\mathrm{Kn}+C_3\mathrm{Kn}^2, \tag{36}$$

where

$$C_1=\frac{a+b}{\sqrt{2\pi}}-\frac{1}{\sqrt{2\pi}}\frac{(b-a)^2\tanh\left(\sqrt{\frac{\pi}{6}}\frac{1}{2\mathrm{Kn}}\right)}{2\sqrt{3}+(a+b)\tanh\left(\sqrt{\frac{\pi}{6}}\frac{1}{2\mathrm{Kn}}\right)}, \tag{37}$$

$$C_2=\frac{8}{\pi}-\frac{8\sqrt{6}}{\pi}\frac{(b-a)\tanh\left(\sqrt{\frac{\pi}{6}}\frac{1}{2\mathrm{Kn}}\right)}{2\sqrt{3}+(a+b)\tanh\left(\sqrt{\frac{\pi}{6}}\frac{1}{2\mathrm{Kn}}\right)}, \tag{38}$$

$$C_3=-\frac{96}{\pi}\sqrt{\frac{2}{\pi}}\frac{\tanh\left(\sqrt{\frac{\pi}{6}}\frac{1}{2\mathrm{Kn}}\right)}{2\sqrt{3}+(a+b)\tanh\left(\sqrt{\frac{\pi}{6}}\frac{1}{2\mathrm{Kn}}\right)}. \tag{39}$$

Here, $Q=\mathrm{Kn}^{-1}\int_{-1/2}^{1/2}\hat{u}_x d\hat{y}$. As $\mathrm{Kn}\to 0$, the asymptotic expression reads

$$Q=\frac{1}{6\mathrm{Kn}}+\left[\frac{a+b}{\sqrt{2\pi}}-\frac{(b-a)^2}{2\sqrt{6\pi}+\sqrt{2\pi}(a+b)}\right]+\left[\frac{8}{\pi}-\frac{1}{\pi}\frac{8\sqrt{6}(b-a)}{2\sqrt{3}+(a+b)}\right]\mathrm{Kn}. \tag{40}$$

For the slip velocity based on the normalized mass flow rate, the first- and second-order slip coefficients for D2Q16 are $c_{1,16}\approx 1.073$ and $c_{2,16}\approx 0.514$, respectively. By applying the same nondimensionalization, the asymptotic solution for the linearized Boltzmann-BGK equation [3] can be written as

$$Q=\frac{1}{6\mathrm{Kn}}+c_{1,\infty}+2c_{2,\infty}\mathrm{Kn}, \tag{41}$$

where the slip coefficients are $c_{1,\infty}\approx 1.147$ and $c_{2,\infty}\approx 0.678$. The higher-order LB scheme D2Q16 gives much improved slip coefficients as compared with the standard D2Q9 scheme, for which the first-order and second-order slip coefficients are $c_{1,9}=\sqrt{6/\pi}(\approx 1.382)$ and $c_{2,9}=4/\pi(\approx 1.273)$, respectively [16].

Figure 1 shows the normalized mass flow rate as a function of Kn. The analytic solution obtained here is confirmed by the numerical solution. For the numerical solution, the DVB equation is discretized by the second-order total variation diminishing (TVD) scheme [25] and the explicit Euler method, and the transverse direction is discretized into 102 lattices including boundary points [26]. As discussed above, D2Q16 gives improved slip coefficients as compared with D2Q9 and is in good agreement with the linearized Boltzmann equation [24] and the direct simulation Monte Carlo (DSMC) method [27] even for the transition regime. Note that as $\mathrm{Kn}\to\infty$, the normalized mass flow rate for D2Q16 approaches a constant value given by

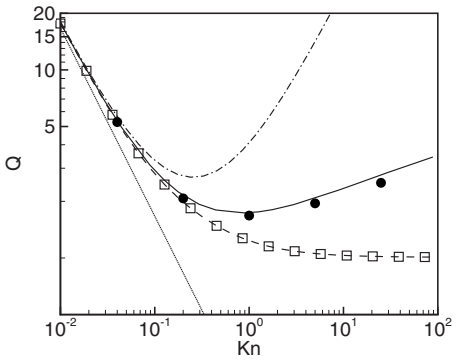

FIG. 1. Normalized mass flow rate (dashed line: D2Q16; squares: numerical solutions for D2Q16; dashed-dotted line: D2Q9; solid line: linearized Boltzmann [24]; circles: DSMC; dotted line: no slip).

$$Q=\frac{5(a+b)}{3\sqrt{2\pi}}-\frac{2(b-a)}{\sqrt{3\pi}}. \tag{42}$$

The constant mass flow rate corresponds to the first-order slip phenomena in Kn—for Navier-Stokes equations with no-slip boundary condition, $Q=1/(6\mathrm{Kn})$. The Knudsen minimum is therefore not reproduced in D2Q16 [26].

IV. MULTIPLE RELAXATION TIME MODEL

In the multiple relaxation time (MRT) model, the relaxation time can have a different value for each moment to relax the limitation of the single relaxation time BGK model. Originally, the LB-MRT model [20,21] has been proposed to improve numerical stability by creating artificially fast dynamics for higher-order moments that do not appear in hydrodynamics at the (isothermal) Navier-Stokes order. Besides the numerics, the relaxation times for the higher-order moments have been used to tune slip velocity in microscale flows [15,16]. In the standard LB method, this phenomenological approach has been adopted to compensate insufficient accuracy in the velocity space discretization for the description of nonequilibrium flows beyond the Navier-Stokes order. In a higher-order LB method, however, the use of a higher-order Gauss-Hermite quadrature to increase the accuracy of velocity space discretization makes the method much more predictive. It is desirable that a higher-order LB-MRT model gives correct relaxation rates dictated by microscopic collision processes. Here, we investigate the effects of the relaxation times for higher-order moments on the slip velocity and the Knudsen layer in the D2Q16 scheme.

The LB-MRT equation for D2Q16 can be written as

$$\partial_t f_i+c_{i\alpha}\partial_\alpha f_i=-\sum_j e_{j,i}^{-1}\frac{m_j^{\mathrm{neq}}}{\tau_j}+F_i. \tag{43}$$

Here, three relaxation times are used: τ for the second- and fifth-order moments, τ_q for the third-order moments, and τ_r for the fourth-order moments. The equations for Q_{xyy} and R_y thus read

$$\partial_y(R_y+3c_s^2P_{xy})=-\frac{1}{\tau_q}(Q_{xyy}-c_s^2j_x)+c_s^2\rho g, \tag{44}$$

$$\partial_y(3c_s^2 Q_{xyy} - 3c_s^4 j_x) = -\frac{1}{\tau_r} R_y. \tag{45}$$

The moments Q_{xyy} and R_y are given by

$$Q_{xyy} - c_s^2 j_x = -\sigma_q(2+3\sigma_r)\tau c_s^2 \rho g - 3\sigma_r\sigma_q \tau^2 c_s^4 \partial_y^2 j_x, \tag{46}$$

$$R_y = 3\sigma_r c_s^2 P_{xy} + 3\sigma_r \tau c_s^4 \partial_y j_x, \tag{47}$$

where $\sigma_q = \tau_q/\tau$ and $\sigma_r = \tau_r/\tau$. The equation for j_x reads

$$-3\sigma^2\tau^3 c_s^4 \partial_y^4 j_x + \tau c_s^2 \partial_y^2 j_x = -\rho g, \tag{48}$$

where $\sigma = \sqrt{\sigma_r \sigma_q}$.

In a similar way to the BGK model, the solution for the velocity is obtained for the MRT model. The normalized velocity for the MRT model is given by

$$\hat{u}_x = -\hat{y}^2 + \frac{1}{4} + \hat{A}_m \phi(\alpha_m \hat{y}) + \hat{B}_m, \tag{49}$$

where

$$\hat{A}_m = -\gamma \frac{2(b-a)/\sqrt{6}\alpha^{-1} + 8/\sqrt{3}\sigma_q \alpha^{-2}}{2\sqrt{3}\gamma\phi(\alpha_m/2) + (a+b)\varphi(\alpha_m/2)}, \tag{50}$$

$$\hat{B}_m = \left[\frac{a+b}{2\sqrt{3}} - \frac{1}{2\sqrt{3}} \frac{(b-a)^2 \varphi(\alpha_m/2)}{2\sqrt{3}\gamma\phi(\alpha_m/2) + (a+b)\varphi(\alpha_m/2)}\right]\alpha^{-1} + \sigma_q\left(\frac{4}{3} - \frac{4}{\sqrt{6}} \frac{(b-a)\varphi(\alpha_m/2)}{2\sqrt{3}\gamma\phi(\alpha_m/2) + (a+b)\varphi(\alpha_m/2)}\right)\alpha^{-2}. \tag{51}$$

Here, $\alpha_m = \alpha/\sigma$ and $\gamma = \sqrt{\sigma_q/\sigma_r}$. The normalized mass flow rate is given by

$$Q = \frac{1}{6\mathrm{Kn}} + C_{1m} + C_{2m}\mathrm{Kn} + C_{3m}\mathrm{Kn}^2, \tag{52}$$

where

$$C_{1m} = \frac{a+b}{\sqrt{2\pi}} - \frac{1}{\sqrt{2\pi}} \frac{(b-a)^2 \tanh\left(\sqrt{\frac{\pi}{6}}\frac{1}{2\sigma\mathrm{Kn}}\right)}{2\sqrt{3}\gamma + (a+b)\tanh\left(\sqrt{\frac{\pi}{6}}\frac{1}{2\sigma\mathrm{Kn}}\right)}, \tag{53}$$

$$C_{2m} = \sigma_q\left[\frac{8}{\pi} - \frac{8\sqrt{6}}{\pi} \frac{(b-a)\tanh\left(\sqrt{\frac{\pi}{6}}\frac{1}{2\sigma\mathrm{Kn}}\right)}{2\sqrt{3}\gamma + (a+b)\tanh\left(\sqrt{\frac{\pi}{6}}\frac{1}{2\sigma\mathrm{Kn}}\right)}\right], \tag{54}$$

$$C_{3m} = -\sigma_q^2 \frac{96}{\pi}\sqrt{\frac{2}{\pi}} \frac{\tanh\left(\sqrt{\frac{\pi}{6}}\frac{1}{2\sigma\mathrm{Kn}}\right)}{2\sqrt{3}\gamma + (a+b)\tanh\left(\sqrt{\frac{\pi}{6}}\frac{1}{2\sigma\mathrm{Kn}}\right)}. \tag{55}$$

As $\mathrm{Kn} \to 0$, the asymptotic expression reads

$$Q = \frac{1}{6\mathrm{Kn}} + \left[\frac{a+b}{\sqrt{2\pi}} - \frac{(b-a)^2}{2\sqrt{6\pi}\gamma + \sqrt{2\pi}(a+b)}\right] + \sigma_q\left[\frac{8}{\pi} - \frac{8\sqrt{6}}{\pi}\frac{(b-a)}{2\sqrt{3}\gamma + (a+b)}\right]\mathrm{Kn}. \tag{56}$$

In the MRT model, the first-order slip coefficient shows dependence on the ratio of the relaxation times for the third- and fourth-order moments. When $\tau_q = \tau$, the first- and second-order slip coefficients increase as the relaxation time for the fourth-order moment decreases. The width and strength of the Knudsen layer are also affected by the relaxation times for the higher-order moments. As $\mathrm{Kn} \to \infty$, the mass flow rate approaches a constant value given by Eq. (42). The asymptotic behavior at large Kn does not change with σ_q and σ_r.

V. CONCLUSIONS

An analysis of a higher-order lattice Boltzmann method is presented with emphasis on the slip velocity and the Knudsen layer. The exact solution of the slip velocity for the LB equation with the D2Q16 velocity set is obtained for Poiseuille flows with finite Knudsen numbers. Due to increased accuracy in velocity space discretization, the higher-order scheme gives much improved slip coefficients as compared with the standard D2Q9 LB method. The Knudsen minimum is, however, not reproduced in the D2Q16 scheme, and the mass flow rate for D2Q16 approaches a constant value in the large Kn limit. The analysis of a MRT model is presented to show the effects of the relaxation dynamics of higher-order moments on the slip velocity and the Knudsen layer.

ACKNOWLEDGMENTS

Financial support by Honda R&D Co., Ltd. Fundamental Technology Research Center, is gratefully acknowledged. The authors would like to thank Professor Iain D. Boyd for providing the DSMC data.

APPENDIX

From Eq. (1), we obtain

$$c_{iy}\partial_y \Phi_i = -\frac{1}{\tau}(\Phi_i - \omega_i \rho), \tag{A1}$$

where

$$\Phi_i = \sum_{c_{jy}=c_{iy}} f_j, \tag{A2}$$

$$\omega_i = \sum_{c_{jy}=c_{iy}} w_j. \tag{A3}$$

At $y = H/2$, $\Phi_i = \Psi\omega_i\rho$ for $c_{iy} < 0$. The solution for Φ_i with $c_{iy} < 0$ can be written as

$$\Phi_i = (\Psi - 1)\omega_i \rho e^{-n/(\tau|c_{iy}|)} + \omega_i \rho, \tag{A4}$$

where n is the distance from the wall in the upstream direction of c_{iy}. Using Eq. (A4), we obtain

$$\Gamma_m = \sum_{c_{jy}<0} |c_{jy}| f_j = (\Psi - 1)\rho c_s (w_a a e^{-n/(a\tau c_s)} + w_b b e^{-n/(b\tau c_s)}) + \rho c_s (w_a a + w_b b). \tag{A5}$$

Due to the symmetry, Ψ at $y=H/2$ is equal to that at $y=-H/2$. At $y=-H/2$, we have

$$j_y|_{y=-H/2} = \Gamma_p|_{y=-H/2} - \Gamma_m|_{y=-H/2} = 0, \tag{A6}$$

where

$$\Gamma_p|_{y=-H/2} = \sum_{c_{jy}>0} |c_{jy}| f_j|_{y=-H/2} = \Psi \rho c_s (w_a a + w_b b). \tag{A7}$$

Therefore, we have $\Psi = 1$.

[1] C.-M. Ho and Y.-C. Tai, Annu. Rev. Fluid Mech. **30**, 579 (1998).
[2] N. G. Hadjiconstantinou, Phys. Fluids **18**, 111301 (2006).
[3] C. Cercignani, *Theory and Application of the Boltzmann Equation* (Scottish Academic Press, Edinburgh, 1975).
[4] G. R. McNamara and G. Zanetti, Phys. Rev. Lett. **61**, 2332 (1988).
[5] Y. H. Qian, D. d'Humières, and P. Lallemand, Europhys. Lett. **17**, 479 (1992).
[6] R. Benzi, S. Succi, and M. Vergassola, Phys. Rep. **222**, 145 (1992).
[7] S. Chen and G. D. Doolen, Annu. Rev. Fluid Mech. **30**, 329 (1998).
[8] S. Succi, *The Lattice Boltzmann Equation for Fluid Dynamics and Beyond* (Oxford University Press, Oxford, 2001).
[9] S. Succi, Phys. Rev. Lett. **89**, 064502 (2002).
[10] S. Ansumali and I. V. Karlin, Phys. Rev. E **66**, 026311 (2002).
[11] F. Toschi and S. Succi, Europhys. Lett. **69**, 549 (2005).
[12] V. Sofonea and R. F. Sekerka, J. Comput. Phys. **207**, 639 (2005).
[13] R. Zhang, X. Shan, and H. Chen, Phys. Rev. E **74**, 046703 (2006).
[14] M. Sbragaglia and S. Succi, Phys. Fluids **17**, 093602 (2005).
[15] L. Szalmas, Physica A **379**, 401 (2007).
[16] S. H. Kim, H. Pitsch, and I. D. Boyd, Phys. Rev. E **77**, 026704 (2008).
[17] S. Ansumali, I. V. Karlin, S. Arcidiacono, A. Abbas, and N. I. Prasianakis, Phys. Rev. Lett. **98**, 124502 (2007).
[18] X. Shan, X.-F. Yuan, and H. Chen, J. Fluid Mech. **550**, 413 (2006).
[19] L. Szalmas, Europhys. Lett. **80**, 24003 (2007).
[20] D. d Humières, I. Ginzburg, M. Krafczyk, P. Lallemand, and L.-S. Luo, Philos. Trans. R. Soc. London, Ser. A **360**, 437 (2002).
[21] P. Lallemand and L.-S. Luo, Phys. Rev. E **61**, 6546 (2000).
[22] S. Ansumali, I. V. Karlin, and H. C. Ottinger, Europhys. Lett. **63**, 798 (2003).
[23] I. V. Karlin and S. Ansumali, Phys. Rev. E **76**, 025701(R) (2007).
[24] C. Cercignani, M. Lampis, and S. Lorenzani, Phys. Fluids **16**, 3426 (2004).
[25] B. van Leer, J. Comput. Phys. **32**, 101 (1979).
[26] S. H. Kim, H. Pitsch, and I. D. Boyd, J. Comput. Phys. (to be published).
[27] G. A. Bird, *Molecular Gas Dynamics and the Direct Simulation of Gas Flows* (Oxford University Press, Oxford, 1994).